UWB Propagation Measurements and Modelling in Large Indoor Environments

CÉSAR BRISO[1], **(Member, IEEE), CESAR CALVO**[1], **AND YOUYUN XU**[2], **(Member, IEEE)**

[1]Technical University of Madrid, ETSIS Telecomunicación, 28031 Madrid, Spain
[2]Nanjing University of Posts and Telecommunications, Nanjing 210028 , China

Corresponding author: Youyun Xu (yyxu@njupt.edu.cn)

ABSTRACT In this paper, we present the results of the measurements and modeling of the propagation channel for ultra wide band (UWB) communications in large indoor environments. The selected environment is a sports center of large dimensions (51×26 m, 7.4m height) without intermediate obstacles so that there is always direct path (DP) between TX and RX and UWB technology can be used for critical communications of sensors. On this environment, narrow band and ultra wide band measurements have been made with a high resolution pulse channel sounder (8ns) at the nominal frequency of 3.9 GHz. Narrow band measurements have been used to model path loss for the DP, while for UWB measurements, the power delay profile have been used to obtain the statistics of the multipath of the channel. Combining both models has been possible to obtain a detailed characterization of the environment. The results constitute a complete characterization of this type of indoor environments for UWB signals and can be easily extrapolated to other environments with similar characteristics, allowing the use of UWB technology for applications of critical communications for sensors and other devices.

INDEX TERMS Channel sounding, channel modeling, critical communications, multipath components, propagation indoor, ultra-wide-band (UWB), wireless sensor networks (WSN).

I. INTRODUCTION

In the last years, Ultra-Wide-Band (UWB) technologies have drawn great interest in wireless communications by allowing reusing part of the existing spectrum for short-range communications. This advantage allows this technology to be used with important benefits for sensor network applications [1]. In this field some of the main industrial applications have been carried out in the field of indoor location [3], personal and short distance sensors [4] and indoor data transmission systems [5]. This latest application has become one of the most promising because it allows the transmission of information from sensors inside medium-sized and large environments such as industrial buildings, hall of stations, airports, shopping centers and others. In these environments, the reliability and immunity to the interference of UWB technology allows us to use this technology to transmit data from critical applications such as fire sensors, alarms and even doors control and other real time applications like critical

sensors [5] or even communications Vehicle to Vehicle (V2V) in a large indoor industrial environment [6]. Nevertheless, critical and real time applications require Direct Path (DP) between Tx and Rx and carefully characterize the channel so that a very precise coverage can be obtained that guarantees the operation of this technology in the whole environment.

We can find some examples of UWB measurements for industrial applications indoors, such as the cabin of a 737 aircraft [8], indoor parking environment [9], industrial working machine [10], in residential and small indoor environments [11] or between vehicles [7]. In these environments, UWB communications are modeled using both, wideband and narrow band measurements as described on [12] or [13]. Using these results, a complete statistical propagation model can be obtained. This model can be improved by using deep learning algorithms [2] to model some special effects such as the influence of density of people [14] or the influence of obstacles [7]. However, we do not find in the literature measurements and a careful modeling of the UWB channel inside large buildings, without walls and other large objects in the interior, such as the hall of stations, airports or

---

The associate editor coordinating the review of this manuscript and approving it for publication was Guan Gui.

TABLE 1. Setup Parameters of Narrow Band Measurements.

Parameter	Value
Measurements tech.	Continuous Wave (CW)
Sampling period	35ms
Measurements speed	100 samp./ wavelength
Center frequency	3.9 GHz
Tx power	29 dBm
Antenna Model	MGRM-WHF (omnidirectional)
Polarization	Linear (V or H)
Antenna Gain	3dBi
Cable + Connec. Loss	3dB
Tx/RX antenna height	1.9m,

shopping centers. Thus, the objective of this paper is to present the UWB measurements made and the modeling of the propagation in this large indoor environment.

The measurements have been carried out in a large sport center, see Fig.1. In this environment, we have carefully measured the propagation and path losses of the channel and statistically modeled the propagation. The results can be applied for the deployment of sensors networks in environments with similar characteristics. Also the model proposed can be used for high capacity communications by using MIMO technology as proposed on [15] and [17], or using special multiple access technology [16].

The paper is organized as follows:

Section II describes in detail the test environment.

Section III, presents narrow-band measurements and a detailed path loss model of the channel.

Section IV presents UWB measurements made with a proprietary channel sounder. These measurements allow modeling of the channel in a bandwidth of 500Mhz. The result is a detailed model of the temporal dispersion and the delay profile of the environment.

Finally, in Section V, results and main conclusions are summarized.

II. INDOOR TESTING ENVIRONMENT

The UWB propagation measurements were performance in an indoor scenario place on Technical University of Madrid (UPM). The scenario is a sport centre, mostly empty without walls or intermediate objects, as can be seen in Fig. 1.
External walls are made of concrete with a steel structure and the roof is made of fiberglass sheet with wavy shape and covered with plasterboards. The building is surrounded by small windows on the top part of the lateral walls. The most remarkable objects are the stands of the public that are made in a staggered way built with bricks and concrete. There are some additional small size elements such as goals and baskets inside the soccer field.

The dimensions of the scenario are some tens of meters. The interior is divided into two environments:

1) Soccer field is a rectangular 45×31 m ($1395m^2$) flat area with 6 steps for the audience along the field with

50cm high and 80cm width. The high roof in this area is 7.4m.

2) Annexed area is an auxiliary area adjacent that is communicated through a window to the field. The dimensions is 6×26m size ($156m^2$) but with a smaller high of 3 m. in Fig.1 it can be seen a photo made in this environment.

The measurement equipment was place on the field, environment. The receiver side was located on a fix position with an antenna on the top of a mast of 1.9m high. On the other hand, the transmitter was mobile equipment with an antenna at same height than receiver. The transmitter described different trajectories depending on the type of measurement done.

III. PATH LOSS MEASUREMENTS AND MODELING

The first step of the characterization of the propagation on a given environment is to obtaining a path loss model of the wide band channel. Nevertheless, in case of UWB systems, this model is highly dependent of the frequency and the signal bandwidth transmitted [18] for this reasons the process of measurements and modelling the channel requires both narrow band measurements and wide band measurements as is described on [12].

Narrow band measurements are used to obtain a path loss model of the indoor channel. This path loss model is useful for UWB systems, coverage planning and, combined with wideband channel sounding measurements, will permit to get an accurate modelling of the environment.

Narrow band measurement have been made on an UWB channel at 3.9 GHz. The test transmitter was a signal generator and power amplifier that sends a continuous wave signal of 29dBm at 3.9GHz. The receiver equipment is a high performance spectrum analyzer MS2830A with a customize software, sampling each 35ms the average power received. The transmitter and receiver antenna used were omnidirectional antennas with 3dB gain and linear polarization. A summary of the parameters of the testbed is given on Table I.

All measurements were carried out with linear and slow constant speed to allow 100 samples per wavelength.
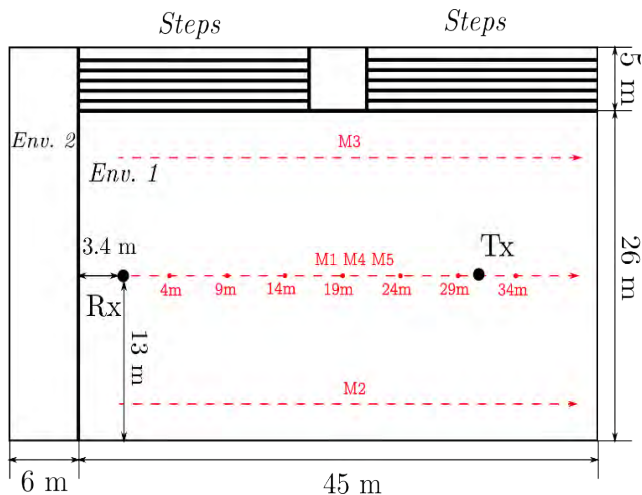
FIGURE 2. Indoor scenario and position of TX and RX during narrow band propagation measurements.
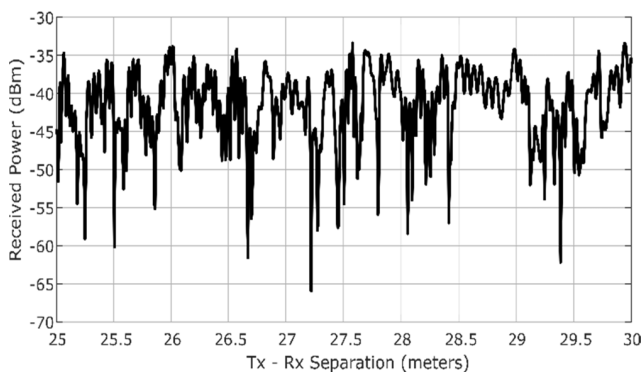

FIGURE 3. Sample of path loss measurements and fast fading at 3.9Ghz moving on M1 trajectory from 25 to 30 m from the receiver.

Measurements were made on several lines M1..M5 moving the transmitter and with the receiver located on a fixed position as shown on Fig. 2. An example of measurements recorded is given on Fig. 3, where we can see the moderate fast fading of the channel. These measurements have been used to obtain a path loss model of the channel for the DP of the transmitted signal.

A. PATH LOSS MODEL

In order to characterize different attenuations and small scale path losses, five measurements have been performance on different trajectories (Fig.2), with vertical, horizontal and cross polarization:

- M1: starts from 1m separation between Tx and Rx and moves away from Rx in the centre of the scenario until the end. The polarization is vertical.
- M2 and M3: were done with vertical polarization, as well. The transmitter was place at 3 m distance form de wall for M2 and 3 m for steps in M3.
- M4 and M5: describe the same trajectory as M1 but the polarization is horizontal and cross polarization, respectively.
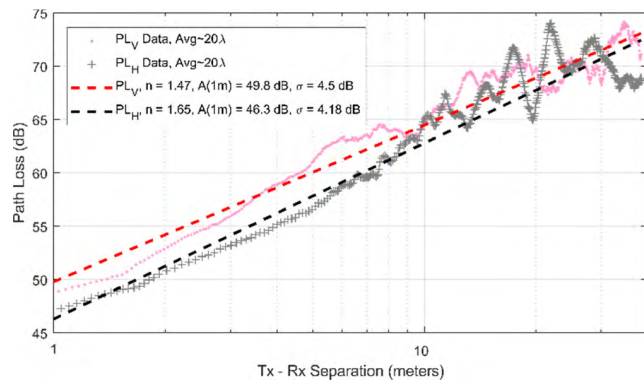

FIGURE 4. 3.9 GHz Indoor Path loss Model for Vertical (red) and Horizontal (black) antenna polarization.

Narrow band analysis it is used to compute the link-budget and to obtain the free space path loss (FSPL) given in the expression:

$$P_{r,FS}(d,f) = P_t + G_t + G_r + 20\log\left(\frac{c}{4\pi df}\right) \quad (1)$$

where P_t is the transmitter power, G_t and G_r are the gain of transmitter (Tx) and receiver (Rx) antennas, respectively. The factor $20\log\left(\frac{c}{4\pi df}\right)$ in (1) is the propagation path loss where d is the distance between Tx and Rx and f, the frequency used.

A straightforward empirical model for single frequency path loss is given by (2).

$$PL(d)[dB] = A(d_0) + 10n \cdot \log\left(\frac{d}{d_0}\right) + X_\sigma \quad (2)$$

where $A(d_0)$ is the attenuation at $d_0 = 1m$ and it can be different to the FSPL at 1m distance; $d > d_0$ is the separation between Tx and Rx and X_σ introduces the large-scale randomness fluctuations over the mean path loss. This parameter is modelled with a zero mean Gaussian random variable in dB.

Fig. 4 shows the path loss model over a logarithmic representation of distance between transmitter and receiver. It compares M1 and M4 (Vertical and Horizontal polarization) that was averaged with 20λ to avoid the fast fading. Its observe that the vertical polarization has slightly higher losses than horizontal polarization. Also path loss exponent in all cases is lower than $n = 2$, which shows that we have a moderate multipath environment.

A summary of the path loss model parameter of all measurement is given in the Table II. This parameters are: $A(d_0)$ is the attenuation at distance $d_0 = 1m$, n is the path loss exponent and X_σ is the standard deviation of a zero mean Gaussian random variable in dB used to model large-scale fading.

B. SMALL-SCALLE FADING

Small scale fading or fast fading gives a qualitative understanding about the multipath propagation effect over the attenuation for a narrow band signal. The fast fading is

TABLE 2. Path loss modelling factors for Narrow band measurements.

$PL(d)[dB] = A(d_0) + 10n \cdot log\left(\frac{d}{d_0}\right) + X_\sigma$				
Measurement	Polarization	n	$A(d_0)$	X_σ
M1: Central	Vertical	1,47	49.78	4.50
M2: Lateral Right	Vertical	1,34	50.95	4.79
M3: Lateral Left	Vertical	1,5	50.30	5.11
M4: Central	Horizontal	1,65	46.29	4.18
M5: Central	Cross-Pol	1,36	58.79	4.93

the rapid fluctuation of power over a short period of time caused by the multipath propagation. It is usually model, on Line of Sight (LoS) conditions, as a random variable with Rician distribution (3) of the envelope amplitude level received, y.

$$P_r(y) = \frac{2(K+1)y}{\Omega} e^{-K - \frac{(K+1)y^2}{\Omega}} I_0\left(2\sqrt{\frac{K(K+1)}{\Omega}}\right) \quad (3)$$

where K is the ratio between the power in the direct path and the power in the NLoS path in natural units. I_0 is the 0th order modified Bessel function of the fist kind. Ω is the total power received, LoS and NLoS.

Have been modeled K factor as a function of distance for the different trajectories M1-M5. To obtain the K factor from narrow band measurements the data values were filter using a moving mean method in order to analyze only the fast fading contribution [20]. Thus, the power received after processing is normalized. Therefore, $\frac{K}{1+K}\Omega = 1$.

Fig. 3 shows a section of 5 meters of the power received where is easy to observe the fast fading contribution with more than 25 dB fades. To measure and model fast fading the raw measurement of the K factor is calculated with a non-overlapping rectangular window of 20cm. Hence, K-factor has a dependence with the T-R Separation with a resolution of 20cm. For each of the 5 measurements done the results are shown in the Fig. 5.

Since the analysis of the results of Fig. 5. show a common trend for all measurements, the K-factor results are model with a linear regression line of the overall contribution of M1 to M5. Although K-factor value is highly influenced by the deterministic LoS component, the behavior does not match with the path loss model. Therefore, its used 2 linear curves fitting split in 2 regions. The regions are from 1m to 10m and from 10m to 40m. thus, K factor can be characterized by the expression in (4).

$$K_{dB} = \begin{cases} a_{1-10} - b_{1-10} \cdot d \, [m] \, if \, 1 \le d < 10 \\ a_{10-40} - b_{10-40} \cdot d \, [m] \, if \, 10 \le d < 40 \end{cases} \quad (4)$$

The results for the five (M1-M5) narrow band measurements are summarized in the Table III. Besides, it was calculated the average of factors *a* and *b* for the contribution of all measurements. See Table III.

TABLE 3. K-factor modelling parameter in function of distance.

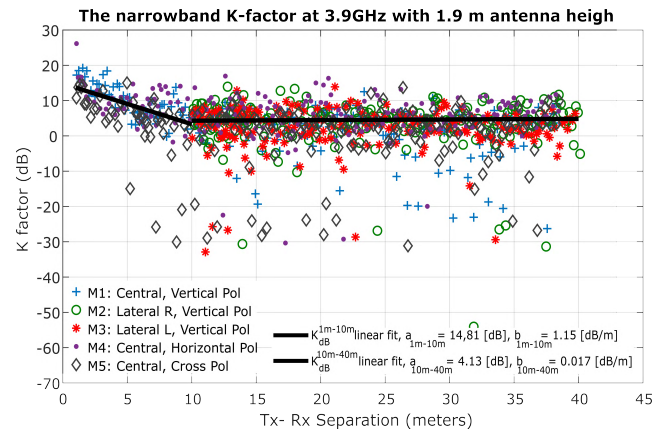| Meas.	$a_{1\text{-}10m}$	$b_{1\text{-}10m}$	$a_{10\text{-}40m}$	$b_{10\text{-}40m}$
M1	17,47	1,41	3,50	0.0466
M2	-	-	4,15	-0,0132
M3	-	-	3,85	0.0449
M4	14,33	0,87	5,55	-0.0301
M5	12.64	1.18	3.60	0.0384
AVG	14.81	1.15	4.13	0.0173

FIGURE 5. Narrowband K-Factor modelling for different antenna polarization and distance of Tx/Rx along the different trajectories (M1-M5).

Some remarks can be drawn from these measures:
- There is not a huge difference between changes in polarization or locations. The most interesting case is M5 in comparison with M1 and M4. Since M5 is expected to have a higher K-factor due to the cross polarization loss of LoS component. Nevertheless, K factor hardly differs from the measures of the rest of co-polarization measurement. This is also coherent with the path loss modelling for the Table III where cross polarization measurement only differs in 8dB.
- The K-factor trend is quite constant when d >10m. One reason could be that when the Tx-Rx separation are small, (d < 10m) the sum of multipath components power (NLoS) are keep constant, whereas when the distance is greater than 10 m the sum of NLoS power decrease slightly with the distance almost like the LoS path loss.
- There is a strong multipath effect. Even when transmitter is near of the receiver K-factor is still low due to this effect.

IV. ULTRA WIDEBAND MEASUREMENTS AND MODELING

UWB propagation models for indoor scenarios have important differences with outdoor propagation. The attenuation is smaller and the influence of the obstacles is different from outdoor. Wide band propagation has been measured in [7] and the influence of obstacles has been described and modeled on [26] for vehicle communications in outdoor environment.

In all cases, a complete modeling of the UWB channel requires channel sounding measurements in the complete indoor environment, and example of this type of measurements is given on [21]. Thus, one effect that must to be take into account is the time dispersion due to the multipath. This indoor environment is specially effected by multipath as described on [22] because there are no scatters in the central space of the environment so that there is a moderate delay spread.

In the following section, we present a complete wideband model for this environment based on delay spread measurements made with an UWB channel sounder.

A. ULTRA WIDEBAND MODEL

The wideband analysis is typically based on measurements of the Power-Delay Profile (PDP) function as described on [19]. This function is an intuitive representation of how much time the signal requires in the propagation to reach the receiver due to the different propagation phenomena as reflections, refractions and scattering, mainly. This function is obtained with some averages of the absolute square value of the channel impulse response (CIR) model which characterized completely the behaviour of the channel. The CIR is the sum of the LoS signal plus the multipath components with different delays and different amplitudes.

Besides, there is an important parameter to quantified: the time dispersion due to the multipath of an environment. The value gives an estimation of the delay τ that is required for the signal to extinguish most of its energy confined. One of the most important and used metric for this parameter is the Root Mean Square Delay Spread (rms-DS) (4)

$$\tau_{rms} = \sqrt{\frac{\sum_0^\infty (\tau - \overline{\tau})^2 \, PDP(\tau)}{\sum_0^\infty PDP(\tau)}} \qquad (5)$$

where $\overline{\tau}$ is the mean excess delay of the channel (5)

$$\overline{\tau} = \frac{\sum_0^\infty \tau \cdot PDP(\tau)}{\sum_0^\infty PDP(\tau)} \qquad (6)$$

B. MEASUREMENT PROCEDURE AND SETUP

There are several techniques for channel sounding and one of the preferred for UWB and indoor scenarios is on the frequency domain by using a Vector Network Analyser. The advantages of the VNA are the possibility of having a very wide band, but this technique is difficult to use on large environments like this because it will require long cable for synchronization and also this technique is not suitable for high number of acquisitions along the all trajectory described by the Tx. So that, the preferred technique for channel sounding of medium size environments is based on the use of a narrow pulse sounder. This technique provide good resolution and is fast and easy to use.

On a pulse sounder the measurement resolution is equal to the bandwidth of the transmitted pulse, and the pulse repetition period should be carefully chosen to allow observation of the time varying response of individual propagation paths,

TABLE 4. Setup Parameters of WideBand Measurements.

Parameter	Value
Sounding Technique	Periodical pulse
Frequency	3.9 GHz
Pulse Shape	Rectangular
Pulse width	8ns
Pulse repetition period	1us
Transmitted bandwidth	>500MHz
Peak power	32 dBm
Power transmitted	10.4 dBm
Antenna Model	MGRM-WHF, omni, Linear polarized
Antenna Gain	3dBi
PDP measuring	1000 PDP/s
PDP averages	100
PDP recording speed	10 PDP/s
Sampling device	R&S RTO2000 Oscilloscope 4GHz Bandwidth 20GS/s

and at the same time to ensure that all multipath components are received between successive pulses. Several UWB channel measurements have been performed using this technique [24], [25], so that we have done time domain measurement using an ad-hoc portable channel sounder developed in the Technical University of Madrid. This equipment is very appropriate for the realization of measurements in close environments of large dimensions, like the one presented on [26].

The channel sounder used for the UWB measurements has the characteristics and configuration described on Table IV. Regarding the pulse width, it defines the bandwidth of the sounding signal. The waveform transmitted is a square pulse of 8ns width that involves an overall bandwidth transmitted higher than 500MHz.

The transmitter power the Tx equipment was set up to transmit peak power of 32dBm. This high power is cause the sounding signal is having high peak to average power ratio characteristics. Thus, the average power transmit is 10.4 dBm. The frequency of the measurements is 3.9 GHz. The antennas used are the same used for narrow band modelling. Model MGRM-WHF, linear polarized covering from 1,1GHz to 6GHz with 3dBi gain and omnidirectional radiation pattern. A complete set of parameters of the sounder is given in the Table IV.

The channel sounder was configured with 1us pulse repetition period measuring. This period was enough to include all
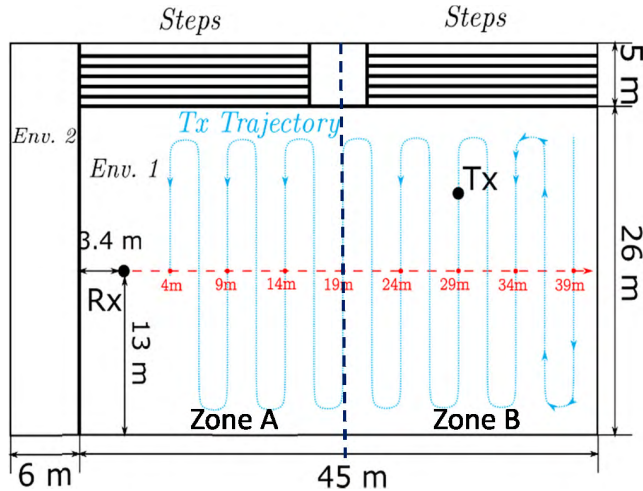
FIGURE 6. Track followed by the channel sounder transmitter during measurements.

FIGURE 7. 3D representation of the power received and delay of multipath components while the channel sounder transmitter is moving following a Zig-Zag trajectory. Y axis is the position on the trajectory.

multipath in the recorded delay profile, because there are no relevant multipath contribution after 500ns of delay. With this configuration, the equipment makes 1000 PDP measurements per second. We configured a periodical average of 100 PDP for each point of measurement to improve accuracy, so that the measuring speed was 10 PDP/second, so it was possible to measure the environment in 20 minutes obtaining 12000 PDP.

The trajectory followed by the transmitter described a zig zag trajectory around the environment 1. The transmitter antenna is on the top of a 1.9 m mast and the system was moving by a person who carried walking with a constant speed. The fig. 6 shows a graphical representation of the trajectory made and the dimensions of the sport centre scenario. This trajectory allow us to characterize all sport centre with an average PDP to see the dependence with distance. In the next section some results are presented.

C. ANALYSIS AND RESULTS

The raw measurements acquired were post processed on *Matlab* and represented on Fig. 7 to provide a qualitative representation of multipath in this environment. The figure shows the 3 dimensional PDP function over the trajectory followed by the TX. The X axis represent excess delay and the Y axis represents the distance followed by the transmitter during the realization of the measurements. That means that the Y axis must be considered only as a reference of the distance covered in the Zig-Zag trajectory followed during the process of measurements described on Fig. 6.

Moreover, the graph has been synchronized in absolute delay in order to avoid the effect of the variation of absolute delay values while the measurement was performance

It can be observed in Fig. 7 some clustering behaviors with the multipath components. We can explain this effect as follows:

- There are some strong cluster reflections bounded in delay from 0 to 88 ns created by the lateral walls
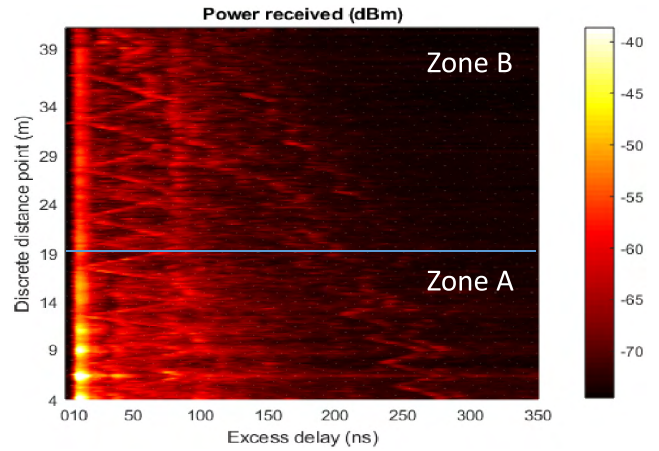
separated 26m. Both lateral reflection measured cross each other because of the path described. One is more strong than the other due to different geometry, while one had steps, the other did not. So, the lateral steps scatter the multipath the received power is smaller.

- Two weak and long reflections bounded in delay from 0 to 277ns that are due to the front and rear walls. Although, geometrically should be 2 crossing diagonals component in measurement of Fig. 7 only can be seen one, which corresponds to the front wall furthest from Rx. The other wall is not a flat wall because has a corridor that connect the environment 1 with the environment 2 (Fig 6.) and the reflection it is weaker and is outside the dynamic range of measurement.

The ground and ceil reflections are no resolvable multipath component then they are mixed with LoS component. These lead in a small fading over the LoS component.

To see more clearly the behavior of the environment analyzed we have defined two zones: zone A for short Tx-Rx distance (<19m) and Zone B for long separation (>19m), These two region can also be identifying in Fig. 7. In these two zones the PDP has been averaged in time to give only one PDP curve that model that area. The results are shown in Fig. 8.

Regarding the time dispersion parameters defined on equations (4) and (5), they have been compute using the same measurements previously analyzed in this section. Thus, the results of Fig. 9 show the value of RMS-DS and mean delay excess of the channel for each one of the PDP taken. For this measurement, the X axis has the same particularity that Fig. 7 has. The axis shows discrete points of distance but is not linear with distance, this distance is the path followed by the transmitter during the measurements.

The values of delay spread measured are between 100ns and 300ns and the main change is due to the LoS power received. That mean the multipath power keep almost constant for all environment, while the variations are produced
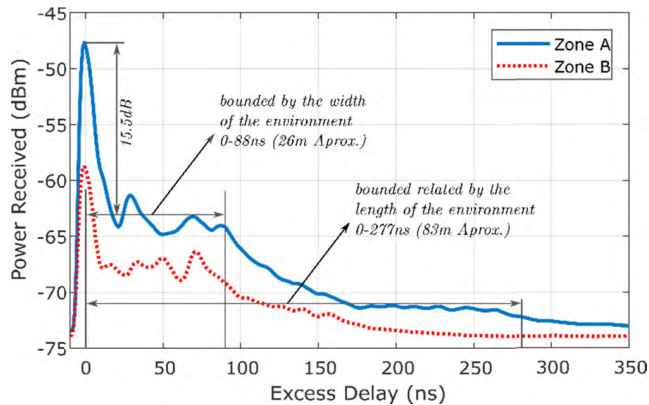
FIGURE 8. Averaged power delay profile measured. Two zones have been defined: Zone A (0-19m) and Zone B (>19m).
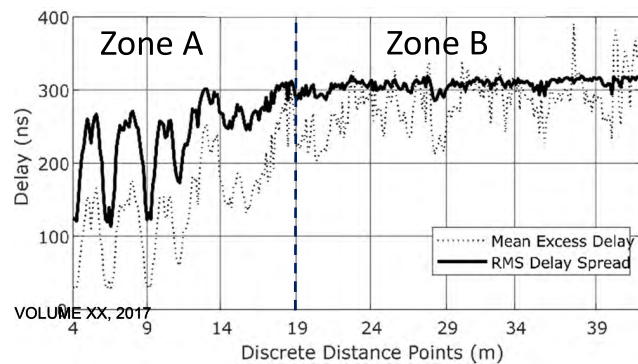
FIGURE 9. RMS Delay spread and mean excess delay along the route followed during the measurements. Two zones defined.

by the direct vision component path loss. This can also be seen on the graph of Fig. 8.

V. CONCLUSIONS

In this paper, UWB propagation has been characterized in large indoor environments with few intermediate walls and objects.

First, narrow-band measurements have been made, and a detailed path loss model has been obtained considering the polarization of the antennas and modelling the fast fading of the channel. This model has an exponent of losses somewhat smaller than "2" as a consequence of the moderate multipath of the environment.

Then the UWB behavior of the channel has been modelled making measurements with a high-resolution channel sounder. These measurements have provided detailed information of the propagation in this type of large environments, where there is a strong clustering effect due to the laterals walls due to the lack of intermediate obstacles.

As a result of this, the multipath is constant in all the environment and the RMS delay is moderate 300ns. However, as a consequence of the variation of the direct path losses, it has been necessary to define two multipath zones, one close to the transmitter where the RMS delay spread varies considerably between 100-300ns and a second zone where it stabilizes at 300ns. Therefore, the PDP can be computed

using the path loss model to calculate the attenuation of the direct path (DP) and adding a constant level of multipath.

The results are useful for the use of UWB signals for the communication of sensor networks for critical applications and for real time applications of industrial machines and devices.

REFERENCES

[1] J. Zhang, P. V. Orlik, Z. Sahinoglu, A. F. Molisch, and P. Kinney, "UWB systems for wireless sensor networks," *Proc. IEEE*, vol. 97, no. 2, pp. 313–331, Feb. 2009.

[2] H. Huang, J. Yang, H. Huang, Y. Song, and G. Gui, "Deep learning for super-resolution channel estimation and doa estimation based massive MIMO system," *IEEE Trans. Veh. Technol.*, vol. 67, no. 9, pp. 8549–8560, Sep. 2018. doi: 10.1109/TVT.2018.2851783.

[3] G. Schroeer, "A real-time UWB multi-channel indoor positioning system for industrial scenarios," in *Proc. Int. Conf. Indoor Positioning Indoor Navigat. (IPIN)*, Sep. 2018, pp. 1–5.

[4] M. Hernandez and R. Kohno, "UWB systems for body area networks in IEEE 802.15.6," in *Proc. IEEE Int. Conf. Ultra-Wideband (ICUWB)*, Bologna, Italy, Sep. 2011, pp. 235–239.

[5] W. Tang and E. Culurciello, "A low-power high-speed ultra-wideband pulse radio transmission system," *IEEE Trans. Biomed. Circuits Syst.*, vol. 3, no. 5, pp. 286–292, Oct. 2009.

[6] R. Reinhold and R. Kays, "Improvement of IEEE 802.15.4a IR-UWB for time-critical industrial wireless sensor networks," in *Proc. IFIP Wireless Days (WD)*, Valencia, Spain, Nov. 2013, pp. 1–4.

[7] R. He, A. F. Molisch, F. Tufvesson, Z. Zhong, B. Ai, and T. Zhang, "Vehicle-to-vehicle propagation models with large vehicle obstructions," *IEEE Trans. Intell. Transp. Syst.*, vol. 15, no. 5, pp. 2237–2248, Oct. 2014.

[8] S. Chiu, J. Chuang, and D. G. Michelson, "Characterization of UWB channel impulse responses within the passenger cabin of a boeing 737–200 aircraft," *IEEE Trans. Antennas Propag.*, vol. 58, no. 3, pp. 935–945, Mar. 2010.

[9] J.-Y. Lee, "UWB channel modeling in roadway and indoor parking environments," *IEEE Trans. Veh. Technol.*, vol. 59, no. 7, pp. 3171–3180, Sep. 2010.

[10] A. Taparugssanagorn, M. Hämäläinen, and J. Iinatti, "Wideband and ultrawideband channel models in working machine environment," *Model. Simul. Eng.*, vol. 2012, Jan. 2012, Art. no. 702917.

[11] S. S. Ghassemzadeh, L. J. Greenstein, A. Kavcic, T. Sveinsson, and V. Tarokh, "UWB indoor delay profile model for residential and commercial environments," in *Proc. IEEE 58th Veh. Technol. Conf. VTC-Fall*, Orlando, FL, USA, vol. 5, Oct. 2003, pp. 3120–3125.

[12] A. Muqaibel, A. Safaai-Jazi, A. Attiya, B. Woerner, and S. Riad, "Pathloss and time dispersion parameters for indoor UWB propagation," *IEEE Trans. Wireless Commun.*, vol. 5, no. 3, pp. 550–559, Mar. 2006.

[13] S. Sangodoyin and A. F. Molisch, "A measurement-based model of BMI impact on UWB multi-antenna PAN and B2B channels," *IEEE Trans. Commun.*, vol. 66, no. 12, pp. 6494–6510, Dec. 2018.

[14] Y.-H. Kim, J.-H. Lee, and S.-C. Kim, "Modeling of UWB channel with population density in indoor LOS environments," *IEEE Antennas Wireless Propag. Lett.*, vol. 15, pp. 1450–1453, 2016.

[15] H. Huang, Y. Song, J. Yang, G. Gui, and F. Adachi, "Deep-learning-based millimeter-wave massive MIMO for hybrid precoding," *IEEE Trans. Veh. Technol.*, vol. 68, no. 3, pp. 3027–3032, Mar. 2019.

[16] G. Gui, H. Huang, Y. Song, and H. Sari, "Deep learning for an effective nonorthogonal multiple access scheme," *IEEE Trans. Veh. Technol.*, vol. 67, no. 9, pp. 8440–8450, Sep. 2018.

[17] H. Jiang, Z. Zhang, and G. Gui, "A novel estimated wideband geometry-based vehicle-to-vehicle channel model using AoD and AoA estimation algorithm," *IEEE Access*, to be published.

[18] A. F. Molisch, "Ultrawideband propagation channels-theory, measurement, and modeling," *IEEE Trans. Veh. Technol.*, vol. 54, no. 5, pp. 1528–1545, Sep. 2005.

[19] Z. Irahhauten, H. Nikookar, and G. J. M. Janssen, "An overview of ultra wide band indoor channel measurements and modeling," *IEEE Microw. Wireless Compon. Lett.*, vol. 14, no. 8, pp. 386–388, Aug. 2004.

[20] R. Shiavi, *Applied Statistical Signal Analysis*. Burlington, VT, USA: Elsevier, 2007.

[21] L. Rubio, J. Reig, H. Fernández, and M. Vicent Rodrigo-Peñarrocha, "Experimental UWB propagation channel path loss and time-dispersion characterization in a laboratory environment," *Int. J. Antennas Propag.*, Mar. 2013, vol. 2013, Art. no. 350167.

[22] N. Alsindi, X. Li, and K. Pahlavan, "Analysis of time of arrival estimation using wideband measurements of indoor radio propagations," *IEEE Trans. Instrum. Meas.*, vol. 56, no. 5, pp. 1537–1545, Oct. 2007.

[23] L. Rusch, C. Prettie, D. Cheung, Q. Li, and M. Ho, "Characterization of UWB propagation from 2 to 8 GHz in a residential environment," *IEEE J. Sel. Areas Commun.*, to be published.

[24] D. Cassioli, M. Z. Win, and A. F. Molisch, "A statistical model for the UWB indoor channel," in *Proc. IEEE VTS 53rd Veh. Technol. Conf.*, Rhodes, Greece, vol. 2, May 2001, pp. 1159–1163.

[25] S. M. Yano, "Investigating the ultra-wideband indoor wireless channel," in *Proc. IEEE 55th Veh. Technol. Conf.*, Birmingham, AL, USA, vol. 3, May 2002, pp. 1200–1204.

[26] L. Zhang *et al.*, "Delay spread and electromagnetic reverberation in subway tunnels and stations," *IEEE Antennas Wireless Propag. Lett.*, vol. 15, pp. 585–588, 2016.

Authors' photographs and biographies not available at the time of publication.

● ● ●